OUKA
The University of Osaka
Institutional Knowledge Archive

Title	Effects of cellular receptors on the vaccine efficacies of adenovirus vector-based vaccines following intramuscular and intranasal administration
Author(s)	Onishi, Rika; Shiota, Aoi; Nakatani, Hayato et al.
Citation	Scientific Reports. 2026, 16, p. 19154
Version Type	VoR
URL	https://hdl.handle.net/11094/106063
rights	This article is licensed under a Creative Commons Attribution-NonCommercial-NoDerivatives 4.0 International License.
Note	

The University of Osaka Institutional Knowledge Archive : OUKA

https://ir.library.osaka-u.ac.jp/

The University of Osaka

scientific reports

Check for updates

OPEN

Effects of cellular receptors on the vaccine efficacies of adenovirus vector-based vaccines following intramuscular and intranasal administration

Rika Onishi[1], Aoi Shiota[1], Hayato Nakatani[1], Masashi Tachibana[1,7], Kahori Shimizu[1], Toshiro Hirai[3,5,6,10], Yasuo Yoshioka[2,3,5,6,10], Fuminori Sakurai[1,8,9]✉ & Hiroyuki Mizuguchi[1,2,3,4]✉

Adenovirus (Ad) vectors are a promising next-generation vaccine modality currently under development. An Ad particle is composed of three major capsid proteins—fiber, penton base, and hexon—that play critical roles in cellular entry. However, the extents to which the receptor-mediated cellular entry pathways influence the efficacy of Ad vector-based vaccines are not well understood. In this study, we examined the effects of the cellular uptake pathway on the vaccine efficacy of Ad vectors by using the β-galactosidase (β-gal)-expressing, capsid-modified Ad vectors that utilize the different cellular entry routes. Following intramuscular vaccination, all capsid-modified Ad vectors induced serum anti-β-gal antibody levels comparable to those induced by the conventional Ad vector. In contrast, after intranasal vaccination, the Ad vectors with mutations in the penton base or hexon elicited anti-β-gal antibody titers in the serum, bronchoalveolar lavage fluid (BALF), and nasal wash at levels comparable with the conventional Ad vector. On the other hand, the coxsackievirus-adenovirus receptor (CAR)-binding-ablated Ad vector exhibited a significant reduction in the anti-β-gal IgG titers in the serum and BALF, and anti-β-gal IgA titers in the BALF and nasal wash. These findings highlight that CAR-mediated transduction is crucial for efficient vaccination with an Ad vector after intranasal administration.

Keywords Adenovirus vector vaccine, Cellular receptor, Capsid modification, Coxsackievirus-adenovirus receptor, αv-integrins, Factor X

The global outbreak of the novel coronavirus disease (COVID-19) has emphasized the critical importance of vaccines in combating infectious diseases worldwide. In particular, the unprecedented speed of vaccine development and clinical application during this pandemic has highlighted the need for vaccine platforms that can be rapidly adapted in response to emerging and re-emerging infectious threats[1,2]. Adenovirus (Ad) vector-based vaccines have emerged as a promising vaccine platform to meet this challenge owing to their favorable characteristics.

[1]Laboratory of Biochemistry and Molecular Biology, Graduate School of Pharmaceutical Sciences, The University of Osaka, 1-6 Yamadaoka, Suita, Osaka 565-0871, Japan. [2]The Center for Advanced Medical Engineering and Informatics, The University of Osaka, Osaka, Japan. [3]Institute for Open and Transdisciplinary Research Initiatives (OTRI), The University of Osaka, Osaka, Japan. [4]Center for Infectious Disease Education and Research (CiDER), The University of Osaka, Osaka, Japan. [5]Research Institute for Microbial Diseases (RIMD), The University of Osaka, Osaka, Japan. [6]BIKEN Innovative Vaccine Research Alliance Laboratories, The University of Osaka, Osaka, Japan. [7]College of Life Sciences, Ritsumeikan University, Shiga, Japan. [8]Laboratory of Biopharmaceutics, Faculty of Pharmacy, Kindai University, Osaka, Japan. [9]Pharmaceutical Research and Technology Institute, Kindai University, Osaka, Japan. [10]Laboratory of Nano, Design for Innovative Drug Development, Graduate School of Pharmaceutical Sciences, The University of Osaka, Osaka, Japan. ✉email: sakurai@phs.osaka-u.ac.jp; mizuguch@phs.osaka-u.ac.jp

Ad vectors offer several advantages for vaccine development: high transduction efficiency; long-term stability at 4 °C; ease of genetic modification—which allows rapid adaptation to various pathogens via a simple exchange of the transgene encoding antigen; and a capacity that permits insertion of large antigen-coding sequences[3–5]. In addition, the Ad vector itself has the ability to act as an adjuvant through its genomic DNA, non-coding VA-RNA, and capsid proteins, thereby activating both innate and adaptive immune responses[6–10]. The cellular entry pathway of Ad vectors is a crucial determinant of the innate immune responses and cellular tropism they elicit[11]. The Ad capsid is primarily composed of three major types of proteins—fiber, penton base, and hexon—each of which plays a distinct role in mediating the initial steps of viral attachment and internalization. The most common Ad vectors are based on Ad serotype 5 (Ad5), which has been widely used as a vaccine vector in both preclinical and clinical studies[12,13]. For Ad5 vectors, Ad fiber first attach to the coxsackievirus-adenovirus receptor (CAR), followed by interaction of the penton base with αvβ3- and αvβ5-integrins, which mediates internalization of the Ad vector through clathrin-dependent endocytosis[14,15]. In addition, coagulation factor X (FX) binds to the hexon protein of Ad, forming a bridge between the viral capsid and heparan sulfate proteoglycans on hepatocytes and other cell types[16–19]. Modifications to capsid proteins, especially the fiber knob and penton base, can significantly alter the vector's cellular entry pathway and immunogenic profile[20,21]. Ablation of CAR-binding via modification of the fiber knob alters the transduction in cells, shifting it from mesothelial cells to liver parenchyma following intraperitoneal administration[22]. Another report showed that an αv-integrin-binding–ablated Ad vector administered intravascularly exhibited reduced spleen uptake and inflammatory activation[23]. Finally, an FX-binding–ablated Ad vector was found to reduce the transduction of hepatocytes after intravenous injection and to attenuate the innate immune activation relative to a the conventional Ad vector[23,24]. However, it remains poorly understood how the infection receptors used for cellular entry of an Ad vector influence the efficacy of Ad vector-based vaccine. Clarifying how infection receptor-dependent entry affects vaccine efficacy is thus essential for rational vector design and for optimizing immune responses through route-specific delivery strategies.

In this study, we examined how receptor-dependent cellular entry pathways affect the efficacy of Ad vector-based vaccines, using three types of Ad vectors with modifications in the capsid proteins critical for cellular binding. Our results showed that although the cellular entry pathway of the Ad vector did not affect the induction of antigen-specific antibody titers after intramuscular administration, CAR-mediated cellular entry was critical for effective vaccination by Ad vectors following intranasal immunization. These findings indicate that CAR binding Ad vectors are preferable for intranasal Ad vector-based vaccines and provide broader insights for the design of intranasal vaccine platforms.

Results

Preparation of capsid-modified Ad vectors

To determine the effects of the infection route of the Ad vectors on the vaccine efficacy, we produced three types of capsid-modified Ad vectors expressing luciferase and β-galactosidase (β-gal) (Table 1, Fig. 1). CAR-binding ablated Ad vectors and αv-integrin-ablated Ad vectors had been developed in our previous study[25]. The CAR-binding ablated Ad vector, Ad/ΔF-LacZ, contained a deletion of four amino acids in the FG loop of the fiber knob region (T489, A490, Y491, and T492). The αv-integrin-binding ablated Ad vector, Ad/ΔP-LacZ, contained a deletion of the RGD (arginine-glycine-aspartate) motif in the penton base. We prepared the FX-binding ablated Ad vectors, Ad/ΔH-Luc and Ad/ΔH-LacZ, which contained the mutations on hypervariable region 7 (HVR7) of the hexon (I421G, T423N, E424S, L426Y and E451Q) referring to Alba R. et al[26]. All the Ad vectors, including the conventional Ad vectors, Ad-Luc and Ad-LacZ, were propagated in HEK293 cells (a human embryonic kidney cell line) and reached comparable titers.

Capsid-modified Ad vector-mediated transduction in vitro

In order to examine whether the mutation in the fiber knob reduced CAR-mediated transduction with Ad vectors, we utilized H1299 (a human non-small cell lung carcinoma cell line) and HepG2 cells (a human hepatocellular carcinoma cell line), which sufficiently express both CAR and αv integrin[27–29]. H1299 and HepG2 cells were transduced with Ad-LacZ, Ad/ΔF-LacZ, Ad/ΔP-LacZ, and Ad/ΔH-LacZ. Ad/ΔF-LacZ showed 16-fold and 115-fold lower transduction efficiency in H1299 cells and HepG2 cells, respectively, compared with conventional Ad-LacZ (Fig. 2A). Ad/ΔP-LacZ showed slightly lower levels of transduction efficiency in H1299 and HepG2 cells compared with Ad-LacZ. In addition, Ad/ΔH-LacZ expressed 1.2-fold and 1.5-fold lower transduction efficiency in H1299 cells and HepG2 cells, respectively, compared with Ad-LacZ. Next, to investigate whether the penton base mutation reduced αv integrin-mediated transduction with Ad vectors, we utilized LN444 cells (a human glioblastoma cell line)[30], which are CAR-negative but αv integrin-positive[27,31]. Ad/ΔF-LacZ showed an approximately eightfold higher transduction efficiency in LN444 cells compared with Ad-LacZ (Fig. 2B). Ad/

Ad vectors	Transgene	Mutation area
Ad-Luc	Luciferase	–
Ad-LacZ	β-galactosidase	
Ad/ΔF-LacZ	β-galactosidase	Fiber
Ad/ΔP-LacZ	β-galactosidase	Penton
Ad/ΔH-Luc	Luciferase	Hexon (HVR7)
Ad/ΔH-LacZ	β-galactosidase	

Table 1. Ad vectors used in this study.

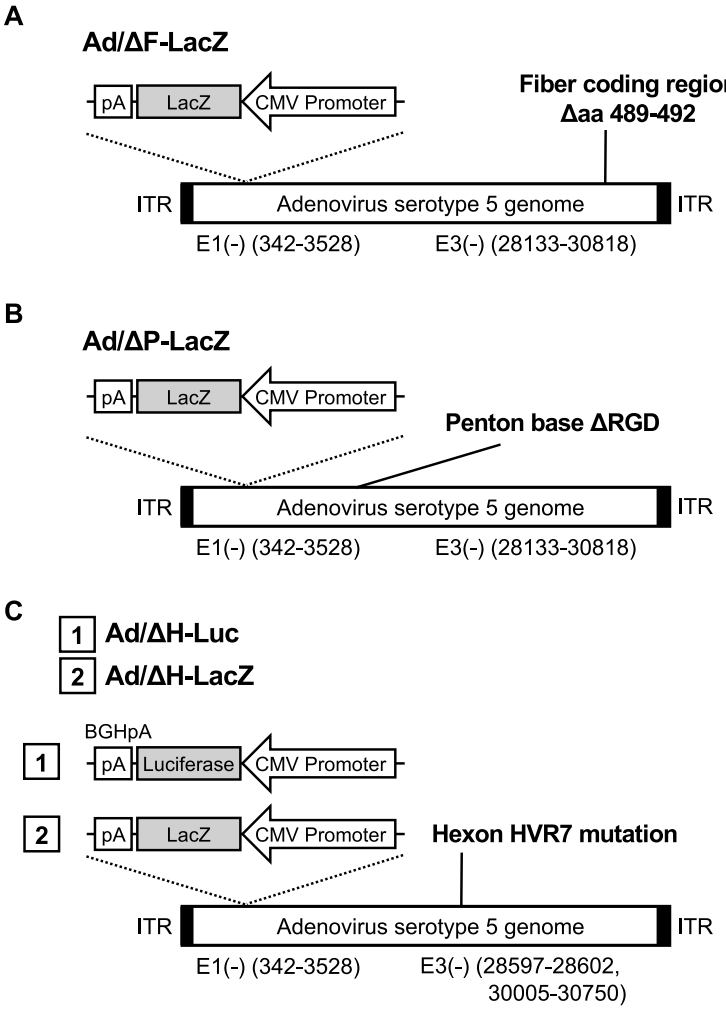


Fig. 1. Schematic diagram of the capsid-modified Ad vectors used in this study. Ad/ΔF-LacZ, a CAR-binding ablated Ad vectors, contain mutations in the FG loop of the fiber protein. Ad/ΔP-LacZ, an αv-integrin-binding ablated Ad vectors, have a deletion of the RGD peptide in the penton base. Ad/ΔH-Luc and Ad/ΔH-LacZ, a FX-binding ablated Ad vectors, have mutations in the HVR7 of the hexon. Either a luciferase or LacZ expression cassette was inserted into the E1-deleted region of the Ad vector genome. CMV, cytomegalovirus immediate-early promoter; Luc, firefly luciferase gene; LacZ, β-galactosidase gene; BGHpA, bovine growth hormone poly A signal.

ΔP-LacZ exhibited a 14-fold lower transduction efficiency in LN444 cells compared with Ad-LacZ. Ad/ΔH-LacZ and Ad-LacZ showed comparable transduction efficiency in LN444 cells.

In order to determine whether the mutation in the hexon led to the ablation of binding to FX, LN444 cells were transduced with Ad/ΔH-LacZ in the absence or presence of FX. Ad-LacZ mediated 6.5-fold higher transduction efficiencies in the presence of FX compared with Ad-LacZ in the absence of FX (Fig. 2C). On the other hand, the transduction efficiency of Ad/ΔH-LacZ did not increase upon addition of FX, suggesting that FX binding to the hexon was successfully ablated in Ad/ΔH-LacZ. Consistent with this finding, reduced luciferase expression was observed in the livers of mice intravenously administered Ad/ΔH-Luc (Supplementary Fig. 1). Ad vectors are known to transduce the liver predominantly via the hexon-FX route after intravenous administration[16,19,32].

Induction of anti-β-gal antibody production after intramuscular administration of capsid-modified Ad vectors

Next, to assess whether the cellular entry pathway of Ad vectors influenced vaccine efficacy after intramuscular administration, we measured the β-gal-specific antibody titers in the serum of mice injected into the bicep femoris muscle with capsid-modified Ad vectors at a dose of 1×10^{10} virus particle (VP)/mouse. The injected dose in this study was comparable or relatively high, compared with those in the previous studies[33–35]. Statistically significant levels of anti-β-gal antibody titers in the serum were detected with all Ad vectors administered, including the capsid-modified Ad vectors, at all serum dilutions tested (Fig. 3A, B). Also, no significant differences in the anti-β-gal antibody titers were observed between conventional Ad-LacZ and the capsid-modified Ad vectors. These results demonstrate that systemic vaccine efficacy was not affected by cellular entry pathways after intramuscular

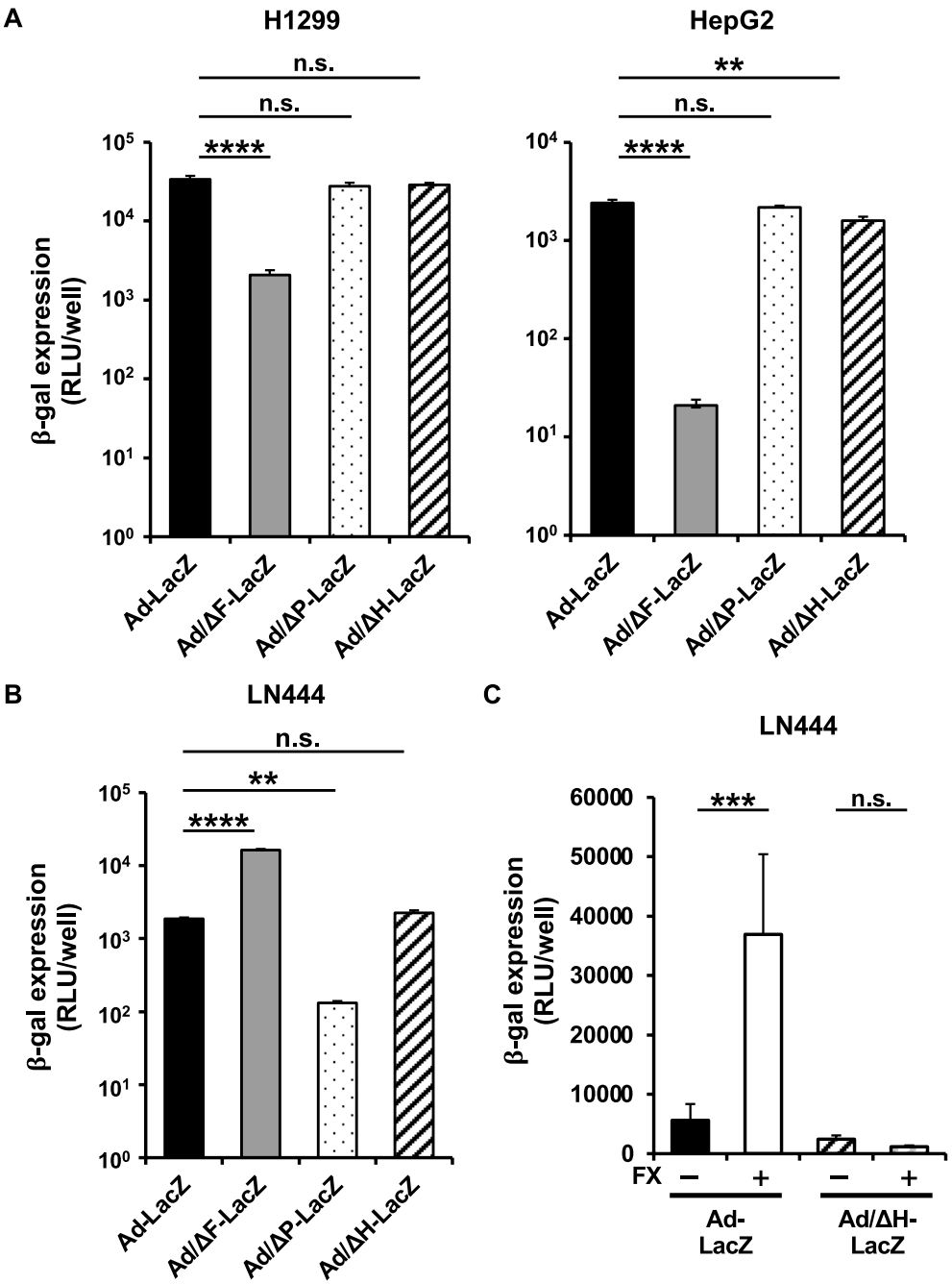


Fig. 2. In vitro transduction efficiency of Ad vectors in human tumor cell lines. H1299 and HepG2 cells were transduced with Ad vectors at 100 VP/cell (A), and LN444 cells were transduced at 3000 VP/cell (B). β-gal activity was measured at 48 h after transduction. For FX-binding analysis, Ad-LacZ or Ad/ΔH-LacZ was pre-incubated with FX (5 μg/mL) before addition to LN444 cells, and β-gal activity was measured after 48 h (C). Data are expressed as means ± S.D. (n = 4). RLU: relative luminescence units. $^{**}p < 0.01$, $^{****}p < 0.0001$ compared with the Ad-LacZ-treated groups. For FX-binding analysis, $^{***}p < 0.01$ compared with the corresponding Ad vector without FX pre-incubation.

administration. The time-course of body weight changes following intramuscular vaccination was similar to that of the PBS-treated group (Supplementary Fig. 2 A). Furthermore, since intramuscular injection is currently the predominant route for Ad vector vaccination in clinical setting, we evaluated cytotoxicity in the muscle to ensure the safety profiles of the modified Ad vectors. Muscle cell toxicity was assessed by measuring levels of creatine phosphokinase (CPK), an enzyme released into the bloodstream when muscle tissue is damaged.

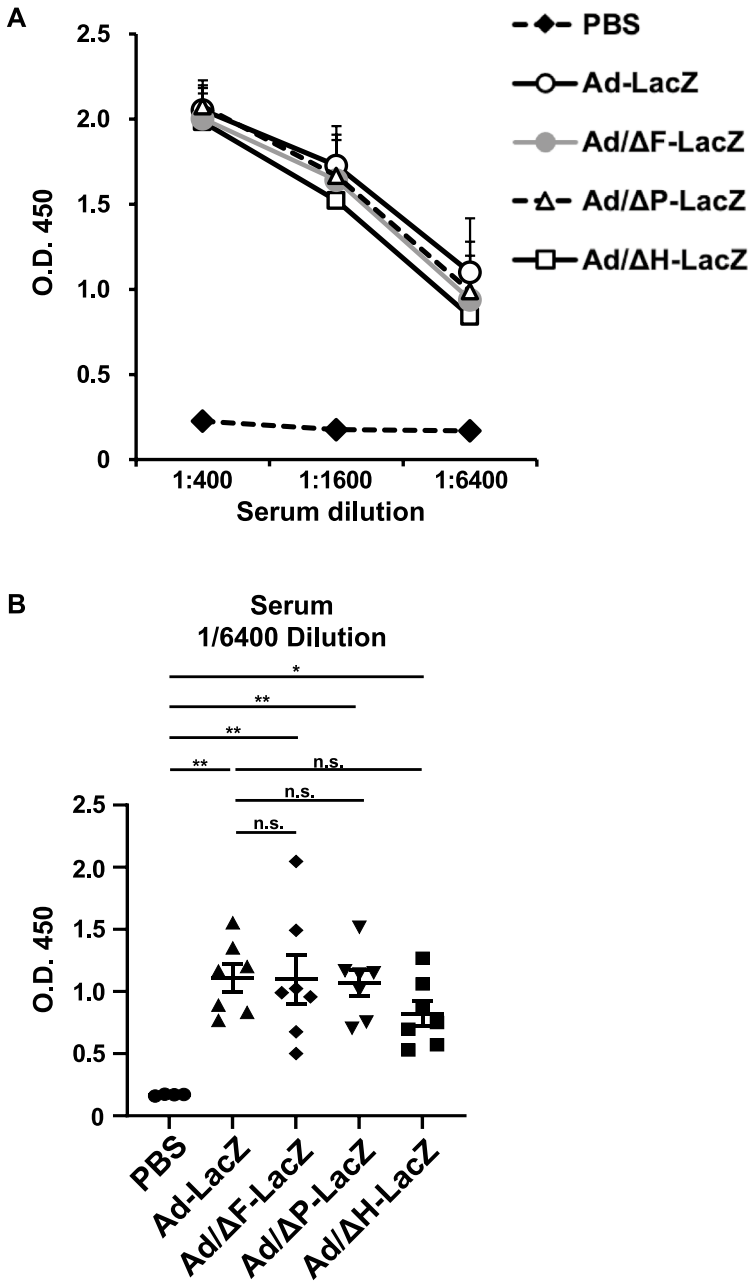


Fig. 3. Anti-β-gal antibody titers in serum following intramuscular immunization with Ad vectors. Mice were intramuscularly administered Ad vectors at a dose of 1.0×10^{10} VP/mouse on day 0 and day 21. Titers of anti-β-gal IgG in serum were evaluated 14 days after the final administration. Anti-β-gal antibody titers were measured at the indicated dilution (A), and antibody titers at serum dilution of 1/6400 are described in (B). The data are represented as means ± SEM (n = 7). $*p < 0.05$, $**p < 0.01$ compared with the PBS or conventional Ad-LacZ treated mice.

All Ad vectors, including the capsid-modified Ad vectors, exhibited the low serum CPK levels comparable to those of PBS-treated mice, indicating that intramuscular injection of Ad vectors did not damage muscle tissue (Supplementary Fig. 3). Collectively, these results suggest that intramuscularly administered Ad vectors exhibit a favorable safety profile.

Transduction efficiencies of capsid-modified Ad vectors in the muscle following intramuscular administration

In order to examine the effects of cellular entry pathways on the transduction efficiencies of Ad vectors in the muscle after intramuscular administration, Ad vectors were intramuscularly administered to mice, and the transduction efficiencies in the muscle were determined 2 days after administration. Significant β-gal production

was not found in the muscle following Ad/ΔP-LacZ administration (Fig. 4A). On the other hand, Ad/ΔF-LacZ and Ad/ΔH-LacZ mediated a high level of β-gal expression at levels comparable to that by conventional Ad-LacZ. These results indicated that αv-integrin binding by the Ad vector was crucial for the transduction in the muscle after intramuscular injection, whereas binding to CAR or FX did not affect the transduction efficiencies in the muscle.

We assessed β-gal expression in other tissues, including the liver and spleen, to determine whether the Ad vector disseminated systemically from the muscle and drove transgene expression following intramuscular administration. None of the Ad vectors mediated significant levels of β-gal expression in the liver or spleen (Supplementary Fig. 4), suggesting the Ad vectors did not disseminate to these organs or mediate transduction after intramuscular administration.

Next, in order to examine the Ad vector accumulation in the muscle, the Ad vector genome copy numbers in the muscle were measured by quantitative PCR analysis. Conventional Ad-LacZ, Ad/ΔF-LacZ, and Ad/ΔH-LacZ exhibited comparable levels of Ad vector genome copies in the muscle after intramuscular administration (Fig. 4B). On the other hand, approximately 5.7-fold lower levels of Ad vector genome copy numbers were found in the muscle following injection of an αv-integrin-ablated Ad vector, Ad/ΔP-LacZ, compared with Ad-LacZ. These results showed the similar tendency with the β-gal expression levels in the muscle, suggesting that Ad/ΔP-LacZ was less efficiently taken up in the muscle and that the numbers of Ad vector genome in the muscle correlates with the transgene expression levels. Taken together, the results indicated that RGD-αv-integrin-binding is important for the gene expression in the muscle after intramuscular administration of an Ad vector; however, transgene expression levels in the muscle did not correlate with the transgene product-specific antibody titers in the serum.

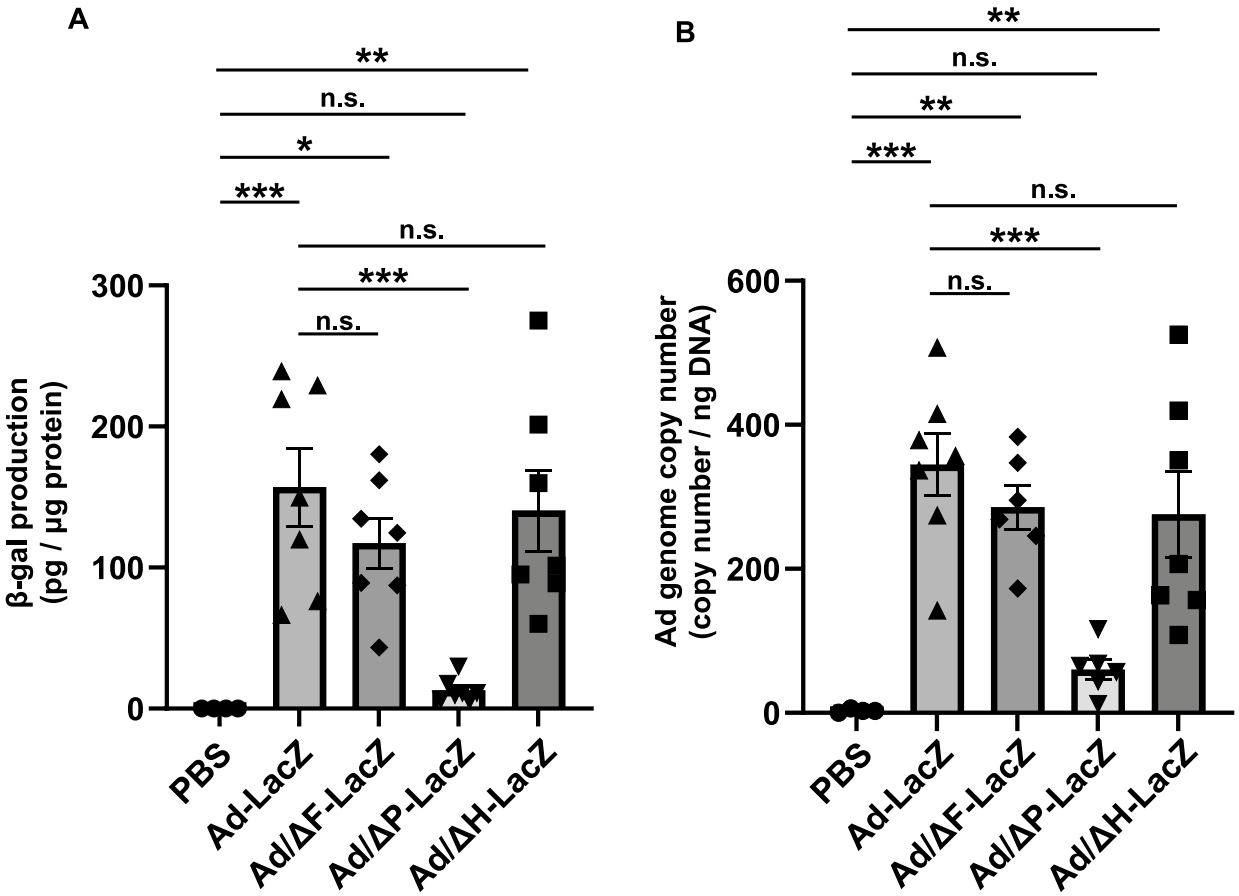


Fig. 4. In vivo transduction efficiencies of Ad vectors in the muscle following intramuscular administration to mice. Ad vectors were intramuscularly administered to mice at a dose of 1.0×10^{10} VP/mouse. β-gal activity levels in the muscle were determined at 48 h after administration (A). Ad genome copy number in the muscle were determined at 48 h after administration (B). These data are expressed as means ± S.E.M. (n = 4–7). $^{*}p < 0.05$, $^{**}p < 0.01$, $^{***}p < 0.001$ compared with the PBS or conventional Ad-LacZ treated mice.

Induction of anti-β-gal antibody production by intranasal administration of capsid-modified Ad vectors

In order to examine the vaccine efficacies of capsid-modified Ad vectors after intranasal immunization, mice were immunized intranasally with the capsid-modified Ad vectors. All modified Ad vectors induced significantly high levels of β-gal-specific IgG in the serum (Fig. 5A). However, anti-β-gal IgG titers in the serum were significantly lower in the mice immunized with Ad/ΔF-LacZ than in those immunized with conventional Ad-LacZ. There were no significant differences in the serum anti-β-gal titers between Ad-LacZ and the other capsid-modified Ad vectors (Ad/ΔP-LacZ and Ad/ΔH-LacZ).

Furthermore, to evaluate the anti-β-gal antibody titers induced at mucosal sites, BALF and nasal wash samples were collected from the mice following immunization with each Ad vector. Similar with the serum IgG results, immunization with Ad-LacZ, Ad/ΔP-LacZ and Ad/ΔH-LacZ induced comparable levels of both

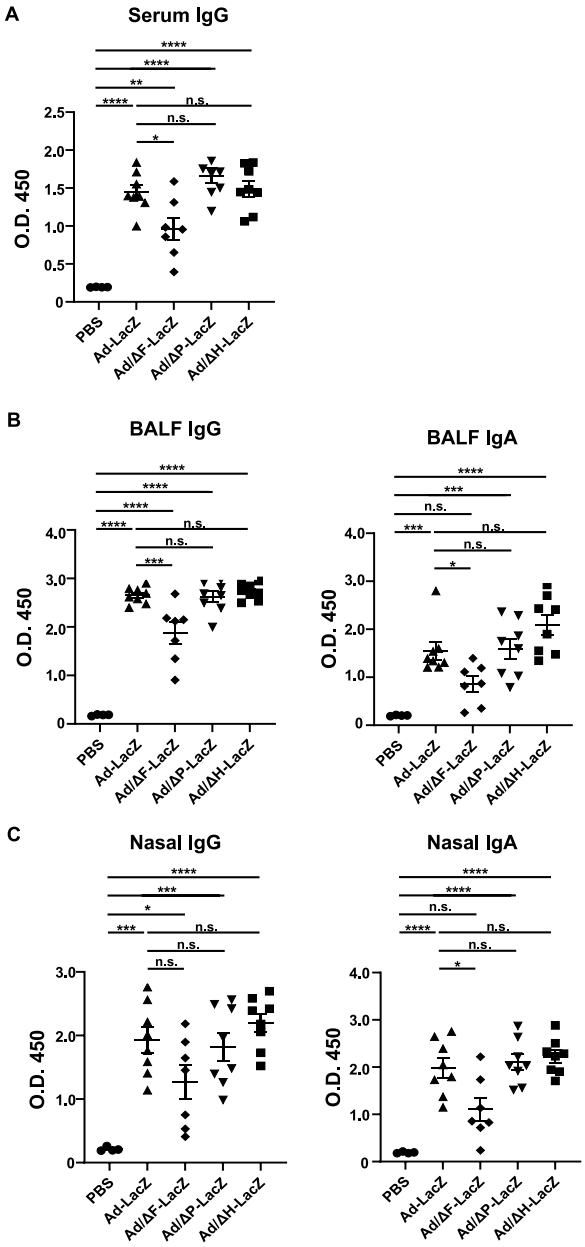


Fig. 5. Anti-β-gal antibody titers in serum, BALF, and nasal wash following intranasal administration of Ad vectors. Mice were intranasally immunized with Ad vectors at a dose of 1×10^{10} VP/mouse on days 0 and 21. Fourteen days after the final administration, anti-β-gal IgG titers were measured in serum diluted 1/6400 (A), anti-β-gal IgG and IgA titers were measured in BALF diluted 1/25 (B), and nasal wash diluted 1/2 (C). The data are represented as means ± SEM. (n = 4–8). $^{*}p < 0.05$, $^{**}p < 0.01$, $^{***}p < 0.001$, $^{****}p < 0.0001$ compared with the PBS or conventional Ad-LacZ-treated mice.

anti-β-gal IgG and IgA in the BALF and nasal wash (Fig. 5B, C). In contrast, Ad/ΔF-LacZ induced significantly lower levels of anti-β-gal IgG and IgA in the BALF compared with conventional Ad-LacZ. Notably, statistically significant differences in anti-β-gal IgA titers were not found in the BALF of PBS-treated and Ad/ΔF-LacZ-immunized mice. Similar trends were observed in nasal wash, where Ad/ΔF-LacZ immunization reduced anti-β-gal IgG and IgA levels, although the reduction in IgG titers did not reach statistical significance compared with Ad-LacZ. Numbers of both $CD4^+$ and $CD8^+$ tissue-resident memory T (T_{RM}) cells were higher in BALF and the lung of Ad-LacZ-immunized mice, compared with those of PBS-immunized mice (Supplementary Fig. 5A, B). In contrast, the numbers of T_{RM} cells in BALF of mice immunized with Ad/ΔF-LacZ were significantly lower than those immunized with conventional Ad-LacZ. There were no statistically significant differences in the numbers of T_{RM} cells in the lung of Ad/ΔF-LacZ and PBS-immunized mice. In addition, numbers of IgA^+ B cells in the lung were significantly lower in the mice immunized with Ad/ΔF-LacZ than in those immunized with conventional Ad-LacZ (Supplementary Fig. 5C). Body weight changes after intranasal vaccination were similar to those of PBS-treated mice (Supplementary Fig. 2B). Taken together, these results suggest that cellular entry via CAR is critical for the induction of transgene product-specific antibody responses in serum IgG, BALF IgG and IgA, and nasal wash IgA following intranasal administration of Ad vector vaccines.

Transduction efficiencies of the capsid-modified Ad vectors in the lung following intranasal administration

To examine whether the reduction in the vaccine efficacy of intranasally administered Ad/ΔF-LacZ was due to the decrease in transduction efficiency, we compared the β-gal expression levels in the lung following intranasal administration of conventional Ad-LacZ and Ad/ΔF-LacZ. Ad/ΔF-LacZ-mediated β-gal expression levels in the lung were significantly lower, at approximately 3.6-fold, than those of conventional Ad-LacZ (Fig. 6A). Similarly, the reduction in the Ad/ΔF-LacZ-mediated transduction efficiencies was also observed in the mRNA levels of the β-gal gene in the lung after intranasal administration of Ad-LacZ and Ad/ΔF-LacZ (Fig. 6B). Furthermore, histochemical analysis using X-gal staining was performed on the lung tissues 24 h after intranasal administration of Ad-LacZ and Ad/ΔF-LacZ (Fig. 6C). In the lungs administered Ad/ΔF-LacZ, only a limited number of X-gal-positive foci were found, whereas lungs receiving Ad-LacZ exhibited more intense β-gal expression with a localized distribution pattern. Collectively, these findings indicate that the fiber-CAR interaction plays a vital role in mediating Ad vector transduction and subsequent vaccine efficacies following intranasal delivery.

Discussion

The aim of this study was to reveal the effects of cellular entry routes of Ad vectors on vaccine efficacy. In this study, we utilized the three types of capsid-modified Ad vectors with mutations in the capsid proteins that are critical for Ad vector internalization to cells (Fig. 1). Utilizing these three Ad vectors, we analyzed in more detail the vaccine efficacies of the Ad vectors following intramuscular and intranasal immunization.

To induce vaccine-mediated immunity, the antigen of interest must first be expressed and presented to the immune system *in vivo*[36]. Intramuscular injection is the most widely adopted route of vaccine administration in the clinical setting[37,38]. Therefore, we first evaluated the transduction efficiencies and vaccine efficacies of the capsid-modified Ad vectors following intramuscular administration. After intramuscular administration of the capsid-modified Ad vectors, the transduction efficiency in the muscle was significantly reduced when cellular entry via αv-integrin was ablated (Fig. 4A). Skeletal muscles are known to express sufficient levels of αv-integrin but low levels of CAR on the cell surface[39–41]; therefore the Ad vector mainly used the RGD peptide on its penton base to be taken up into muscle cells. In our previous report, the insertion of the RGD peptide on the fiber knob of Ad serotype 35 had significantly improved its transduction efficiency in the muscle tissue, suggesting that the RGD peptide is important for the Ad vector-mediated transduction in the muscle[42].

Although an αv-integrin-ablated Ad vector, Ad/ΔP-LacZ, showed significant reduction in its transgene expression levels in the muscle following intramuscular administration, the antigen-specific antibody IgG titers induced by intramuscular immunization of the capsid-modified Ad vectors, including Ad/ΔP-LacZ, were comparable to those of conventional Ad-LacZ (Fig. 3B). It remains unclear why Ad/ΔP-LacZ induced the antigen-specific antibody IgG titers at levels comparable to the other Ad vectors, even though the transduction efficiency of Ad/ΔP-LacZ in the muscle was relatively low. It is possible that the β-gal expression levels at this dose (1×10^{10} VP/mouse) of the Ad vectors in this study caused a saturation of anti-β-gal antibody production, and that high titers of anti-β-gal antibody was produced even with the lower transduction efficiency of Ad/ΔP-LacZ, compared with those of the other Ad vectors. Another possible explanation could be that the cells transduced with Ad/ΔP-LacZ via an αv-integrin-independent pathway played an important role in the induction of the antigen-specific antibody titers. An Ad vector mainly transduces muscle fiber cells, which are αv-integrin-positive but express low levels of CAR, following intramuscular administration[41]. In the present study, Ad/ΔP-LacZ was not found to efficiently transduce muscle fiber cells after intramuscular administration. Collectively, these results indicate that the level of transgene expression by Ad vectors in muscle fibers did not correlate with the antigen-specific antibody IgG titers.

Intranasal vaccines are gaining significant attention because they can induce both systemic and respiratory mucosal immune responses, which are essential for preventing pathogen entry at mucosal surfaces[43–45]. In contrast, intramuscular vaccines can effectively induce systemic immune responses, but are generally ineffective at eliciting sufficient mucosal immunity. Ad vector-based vaccines are well suited to intranasal vaccination. Recent studies have reported that intranasal administration of rhesus adenovirus-derived Ad vector vaccines elicited superior mucosal immune responses, compared with mRNA vaccines[46–48]. In this study, intranasal administration of Ad-LacZ resulted in efficient induction of transgene-specific IgG and IgA at the mucosal surface. In contrast, intranasal administration of Ad/ΔF-LacZ led to an apparent reduction in antigen-specific IgG antibody titers in the serum and BALF compared with conventional Ad-LacZ (Fig. 5A, B). Moreover, no

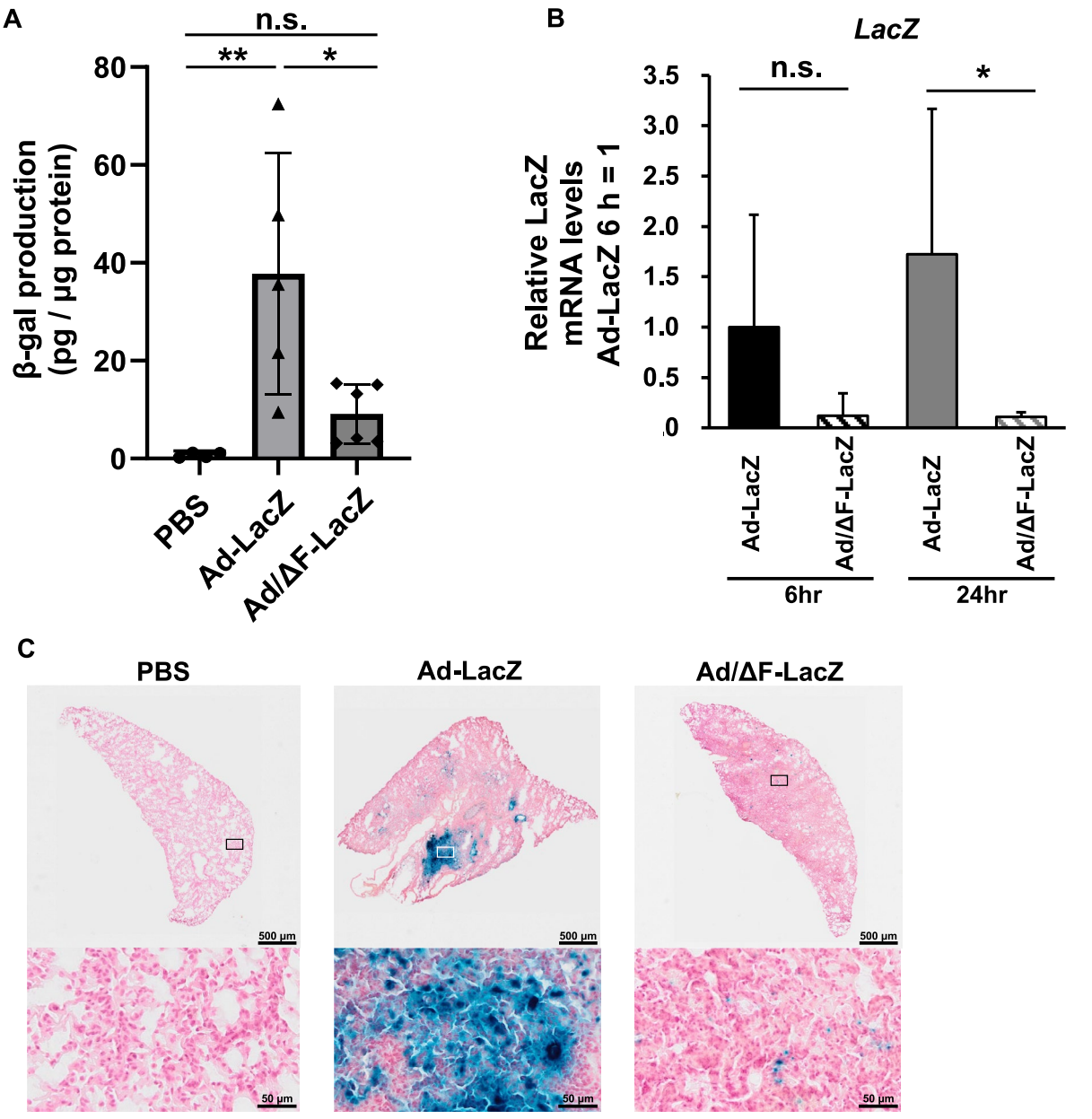


Fig. 6. In vivo transduction efficiencies in the lung following intranasal administration of Ad vectors. Ad-LacZ and Ad/ΔF-LacZ were intranasally administered to mice at a dose of 1.0×10^{10} VP/mouse. β-gal activity in the lung and X-gal staining of lung tissues were assessed at 24 h after administration (A, C). Relative LacZ mRNA levels in the lung were measured at the indicated time points (B). The relative LacZ mRNA levels of the Ad-LacZ-treated group measured at 6 h following administration was normalized to 1. These data are expressed as means ± S.E.M. (n = 4–6). $^{*}p < 0.05$, $^{**}p < 0.01$.

statistically significant elevation of antigen-specific IgA antibody was observed in the BALF or nasal wash of mice immunized with Ad/ΔF-LacZ. The significant reduction of BALF IgA titers in the mice immunized with Ad/ΔF-LacZ, compared with conventional Ad-LacZ, can be attributed to the decrease of IgA^+ B cells (Supplementary Fig. 5 C).

Even though we focused mostly on humoral immune response as the primary correlate of protection in this study, it is well known that Ad vector vaccines induce T cell activation[12,49]. The magnitude of the initial T cell expansion and the number of subsequent memory T cells are directly correlated with the antigen load[50]. Therefore, the reduction in β-gal expression in the lung of Ad/ΔF-LacZ-immunized mice likely led to the reduction in the numbers of T_{RM} cells in both BALF and the lung (Supplementary Fig. 5 A, B). In addition, $CD4^+$ T cells are critical for Ad vector-induced immunity, since $CD4^+$ T cells play an important role in both robust antibody production[51,52] and the maintenance of functional $CD8^+$ T cell responses[53]. Since the numbers of $CD4^+$ T_{RM} decreased following intranasal administration of Ad/ΔF-LacZ, compared with Ad-LacZ, this may have led

to the significant reduction of antigen-specific antibody titers following intranasal administration of the CAR binding-ablated Ad vector, compared with conventional Ad vector. Taken together, these findings suggest that transduction of CAR-positive cells in the lung is important for inducing antigen-specific antibody titers and the T cell response following intranasal administration of an Ad vector.

CAR-binding Ad vector vaccines showed elicited effective antigen-specific antibody titers following intranasal administration. Currently, clinically approved intranasal Ad vector vaccines, such as Convidecia Air in China and Sputnik V in Russia, both of which use CAR for entry, have been shown to efficiently induce transgene-specific antibody production[54,55]. Another approved intranasal Ad vector vaccine, iNCOVACC from India, is based on chimpanzee Ad serotype 36 (ChAd36)[33,56]. Although the cellular receptor for ChAd36 has not yet been identified, ChAd36 and chimpanzee Ad Y25—the backbone of ChAdOx1[57]—, belong to the same species, simian Ad species E[35]. ChAdOx1 has been shown to utilize CAR as a high-affinity receptor[58]. It is therefore plausible that ChAd36 also employs CAR for entry. Taken together, these observations suggest that CAR-mediated delivery of Ad vector vaccines is crucial for the efficacy of intranasally administered Ad vector vaccines.

Vaccine-induced immune thrombotic thrombocytopenia (VITT) is a concern associated with the use of Ad vector-based vaccines, as rare but severe thrombotic events have been reported following vaccination with ChAdOx1 and Ad26.COV2.S[59–61] A recent study reported that the RGD motif on penton base directly interact with platelet integrin αIIbβ3, resulting in a mechanistic link to thrombosis[62]. Since many Ad serotypes contain the penton RGD motifs[21,63], this finding implies that thrombotic risk may not be restricted to ChAdOx1 but could be a broader concern for other serotype-based Ad vector vaccines containing the penton RGD motif. In this study, deletion of the RGD on the penton base did not significantly impair the anti-β-gal antibody induction following either intramuscular or intranasal immunization. These data suggest that modified Ad vector vaccines lacking the penton RGD motif are a promising framework as a vaccine vector because Ad vector-induced thrombotic risk is minimized.

A limitation of the present study is that we did not examine the contributions of distinct cell populations within the muscle tissue following intramuscular administration of Ad vectors. The muscle microenvironment is composed of not only the muscle cells but also of resident immune cells[64], which are considered to be involved in vaccine efficacies. Evaluating the transduction efficiencies and subsequent activation of these immune cell subsets following intramuscular administration of modified Ad vectors remains important for future investigations.

In summary, we demonstrate that, although the cellular entry pathway does not significantly influence antigen-specific IgG titers in serum after intramuscular administration of Ad vector vaccines, CAR-mediated cellular entry is important for Ad vector-mediated effective vaccination following intranasal immunization. These findings offer valuable insights for the development of intranasal vaccine platforms.

Materials and methods

Cell lines

HEK293A (Thermo Fisher Scientific, San Jose, CA), HepG2 (RCB1648, JCRB Cell Bank, Tokyo, Japan), and LN444 cells (kindly provided by Dr. Tada, Hokkaido University, Hokkaido, Japan)[30] were cultured with Dulbecco's modified Eagle's medium (DMEM) supplemented with 10% fetal bovine serum (FBS), 2 mM glutamine, and antibiotics. H1299 cells (American Type Culture Collection, Manassas, VA) were cultured with RPMI-1640 supplemented with 10% FBS and antibiotics. All cells were cultured at 37℃ in 5% CO_2 atmosphere.

Development of Ad vector plasmids

The Ad vector plasmid, pAdHM309-HVR7.1, was constructed according to the strategy of Alba et al.[24] and used to generate the FX-binding–ablated Ad vector. Briefly, the peptide motif in HVR7 of the hexon, GGVINTETLTKVKPKTGQENGWEKDATEFSDKNE, was changed into GGVGNNSTYTKVKPKTGQENGWEKDATEFSDKIE (mutated amino acids are underlined), resulting in pAdHM309-HVR7.1. I-*Ceu*I/PI-*Sce*I-digested pAdHM309-HVR7.1 was ligated with I-*Ceu*I/PI-*Sce*I-digested pCMVL1 and pHMCMVLacZ2[65], which contained a cytomegalovirus (CMV) promoter-driven firefly luciferase or β-gal expression cassette, respectively, obtaining pAdHM309-HVR7.1-CMVL2 and pAdHM309-HVR7.1-CMVLacZ2. CAR- or αv-integrin-binding ablated Ad vector plasmids expressing β-gal were similarly constructed using pAdHM26 and pAdHM32[25], respectively, obtaining Ad/ΔF-LacZ and Ad/ΔP-LacZ. The luciferase-expressing Ad vector plasmids for a conventional Ad vector, Ad-Luc (same as Ad-L2 in the previous study), a CAR-binding ablated Ad vector, were previously constructed[25,66]. A β-gal-expressing conventional Ad vector plasmid for Ad-LacZ (same as Ad5-LacZ in the previous study) had also been constructed previously[42]. Details of the plasmid construction methods are available upon request.

Preparation of Ad vectors

All Ad vectors were constructed by means of an improved in vitro ligation method described previously[65,67]. Ad vector plasmids were digested with *Pac*I and transfected into HEK293 cells using Lipofectamine 2000 (Thermo Fisher Scientific, San Jose, CA). All Ad vectors were propagated in HEK293 cells, purified by two rounds of cesium chloride-gradient ultracentrifugation, dialyzed, and stored at −80 °C. The VP titers were determined by the method of Maizel *et al*[68].

Ad vector-mediated transduction into cultured cells

Cells were seeded at 1×10^4 cells/well onto a 96-well plate. On the following day, the cells were transduced with Ad-LacZ, Ad/ΔF-LacZ, Ad/ΔP-LacZ, and Ad/ΔH-LacZ at 100 VP/cell (for H1299 and HepG2 cells) or at 3000 VP/cell (for LN444 cells). After 48 h of incubation, β-gal production in the cells was determined using a Galacto-Light Plus β-galactosidase reporter gene assay system (Thermo Fisher Scientific). For the analysis of FX binding

to Ad vector, Ad-LacZ and Ad/ΔH-LacZ were incubated with human FX (Prolytix, Essex Junction, VM) at the concentration of 5 μg/mL for 1 h at room temperature, and then were added to LN444 cells at 3000 VP/cell. After a 48-h incubation, β-gal expression in the cells was determined as described above.

Ad vector-mediated transduction efficiency in mice following intramuscular and intranasal administration

Ad-LacZ, Ad/ΔF-LacZ, Ad/ΔP-LacZ, and Ad/ΔH-LacZ (1×10^{10} VP/50 μL/mouse) were intramuscularly administered to C57BL/6 J mice (female, 6 weeks old) (Japan SLC Co. Ltd., Shizuoka, Japan), which are anesthetized with 2% isoflurane (FUJIFILM Wako Pure Chemical, Osaka, Japan). Mice were euthanized by inhalation of 5% isoflurane until respiratory arrest, and the muscles were isolated from the mice at 48 h after administration and homogenized, followed by three rounds of freezing and thawing. The homogenates were then centrifuged at 21,900 × g for 15 min at 4 °C. β-gal expression in the supernatants was measured using the Galacto-Light Plus β-galactosidase reporter gene assay system (Thermo Fisher Scientific). To evaluate the transduction efficiencies of Ad vectors in the lung, Ad-LacZ and Ad/ΔF-LacZ (1×10^{10} VP/30 μL/mouse) were administered intranasally to mice. The lungs were isolated from the mice at 24 h after administration and homogenized, followed by three rounds of freezing and thawing. The β-gal activity in the supernatants was similarly measured as described above. The protein concentration in the supernatants was measured with a Bio-Rad Protein Assay Kit (Bio-Rad, Hercules, CA) using bovine serum albumin as a standard.

In vivo imaging of Ad vector-mediated luciferase expression in mice

Mice were anesthetized with 2% isoflurane, and Ad vectors were administered intravenously at a dose of 1×10^{10} VP/mouse. Forty-eight h after administration, mice were intraperitoneally administered D-luciferin potassium salt (FUJIFILM Wako Pure Chemical), as a luciferase substrate, at a dose of 3 mg/mouse. Fifteen minutes later, mice were imaged using a NightOWL II LB 983 in vivo imaging system (Belthold Technologies, Bad Wildbad, Germany). Luciferase activity was visualized as pseudocolor images, with the maximum signal shown in light blue and the minimum in blue.

Ad vector-mediated vaccination of mice following intramuscular or intranasal administration

Mice were anesthetized with 2% isoflurane, and Ad-LacZ, Ad/ΔF-LacZ, Ad/ΔP-LacZ, and Ad/ΔH-LacZ were intramuscularly (1×10^{10} VP/50 μL/mouse) or intranasally (1×10^{10} VP/30 μL/mouse) administered to C57BL/6 J mice (female, 6-weeks old) on days 0 and 21. Mice were euthanized by inhalation of 5% isoflurane until respiratory arrest on day35. On day 35, anti-β-gal antibody titers in the serum, bronchoalveolar lavage fluid (BALF), and nasal wash were determined by ELISA. In brief, the ELISA plates were coated with recombinant β-gal (1 μg/mL) (Sigma-Aldrich, St. Louis, MO) in carbonate buffer overnight at 4 °C and then incubated with fivefold diluted ImmunoBlock (DS Pharma Biomedical, Osaka, Japan) for 1 h at room temperature. Serum, BALF, and nasal wash samples, diluted in 20-fold diluted ImmunoBlock, were added to the antigen-coated plates. After incubation for 2 h at 37 °C, the coated plates were incubated with a goat anti-mouse IgG (H + L)-BIOT (dilution 1:5000; Southern Biotech, Birmingham, AL) or goat anti-mouse IgA (H + L)-BIOT (dilution 1:5000; Southern Biotech) as secondary antibodies for 2 h at 37 °C. Finally, the plates were incubated with a horseradish peroxidase (HRP)-labeled streptavidin (dilution 1:5000; Southern Biotech), for 1 h at room temperature. The color reaction was developed using a Substrate Reagent Pack (catalog numbers: DY999, R&D System, Minneapolis, MN), stopped with 0.5 N HCl, and the absorbance was measured at OD450 on a plate reader.

Quantitative PCR analysis

Ad vectors were intramuscularly administered as described above. Mice were euthanized by inhalation of 5% isoflurane until respiratory arrest, and the tissues were isolated at 48 h following Ad vector administration. Total DNA, including Ad genomic DNA, was extracted from the muscles by using DNAzol (Molecular Research Center, Cincinnati, OH). The Ad genome copy numbers were quantified by PCR analysis (StepOnePlus System, Thermo Fisher Scientific) using the primers for the Ad5 E4 genes[69], and THUNDERBIRD Next SYBR qPCR Mix reagents (TOYOBO, Osaka, Japan). The values were normalized by the copy numbers of a housekeeping gene, mouse glyceraldehyde-3-phosphate dehydrogenase (GAPDH).

Ad vectors were intranasally administered as described above. Mice were euthanized by inhalation of 5% isoflurane until respiratory arrest, and the lungs were isolated at 6 or 24 h following Ad vector administration, followed by RNA isolation using Isogen (Nippon Gene, Tokyo, Japan). Real-time RT-PCR analysis was performed using THUNDERBIRD Next SYBR qPCR Mix reagent and a StepOnePlus System. The values were normalized by the mRNA levels of a housekeeping gene, mouse GAPDH. The sequences of the primers are available on request.

β-gal staining of the lung following intranasal administration of Ad vectors

Fresh tissues were embedded in O.C.T. compound (Sakura Fintech, Tokyo, Japan), snap-frozen, and stored at −80 °C. Tissues were sectioned at 7 μm thickness using a cryostat (Leica, Nussloch, Germany). Prior to staining, tissue sections were fixed in cold 0.5% glutaraldehyde diluted in PBS for 10 min and incubated with β-gal staining solution (2% X-gal, 30 mM potassium ferrocyanide, 30 mM potassium ferricyanide, 1 M $MgCl_2$, 5 M NaCl, 0.5 M HEPES) overnight at 37 °C. The following day, the sections were washed three times with PBS, then counterstained with nuclear fast red-aluminum sulfate solution (Sigma-Aldrich) for 5 min at room temperature. After washing in PBS for 5 min, the sections were dehydrated in a graded ethanol series and cleared in xylene. After drying, the samples were examined under a microscope.

Flow cytometry

The lungs were surgically excised and incubated in 2% FBS/PBS supplemented with DNase I (New England Biolabs, Ipswich, MA) and collagenase type I (Fujifilm Wako Pure Chemical) at 37°C for 80 min. The digested lungs were dissociated by extrusion through a 70 μm cell strainer (AS ONE, Osaka, Japan) and washed with 2% FBS/PBS. After red blood cells were lysed, the lung lymphocytes were collected using Lympholyte-M (CEDARLANE, Burlington, ON, Canada) according to the manufacturer's instructions. Isolated cells were stained and analyzed using MACSQuant Analyzer (Miltenyi Biotec, Bergisch Gladbach, Germany) as described in our previous study[70]. The fluorescently labeled antibodies used for flow cytometry are listed in Supplementary Table 1.

Statistical analyses

Two-tailed unpaired Student's t-test, one way-ANOVA, or two way-ANOVA followed by Tukey's post hoc test, Dunnett's post hoc test, or Bonferroni's post hoc test was used for statistical analyses. These analyses were conducted using Graph Pad Prism software (GraphPad Software, San Diego, CA). Data are presented as means ± SD or SEM.

Data availability

The datasets generated during and/or analyzed during the current study are available from the corresponding author on reasonable request.

Received: 30 September 2025; Accepted: 13 April 2026
Published online: 25 April 2026

References

1. Krammer, F. Pandemic vaccines: How are we going to be better prepared next time?. *Med* **1**, 28–32 (2020).
2. Lurie, N., Saville, M., Hatchett, R. & Halton, J. Developing Covid-19 vaccines at pandemic speed. *N. Engl. J. Med.* **382**, 1969–1973 (2020).
3. Sakurai, F., Tachibana, M. & Mizuguchi, H. Adenovirus vector-based vaccine for infectious diseases. *Drug Metab. Pharmacokinet.* **42**, 100432 (2022).
4. Hackett, N. R. & Crystal, R. G. Four decades of adenovirus gene transfer vectors: History and current use. *Mol. Ther.* **33**, 2192–2204 (2025).
5. Murala, M. S. T., Gairola, V., Sayedahmed, E. E. & Mittal, S. K. Next-generation adenoviral vector-based vaccines for severe acute respiratory syndrome Coronavirus-2. *Vaccines* **13**, 406 (2025).
6. Hartman, Z. C., Appledorn, D. M. & Amalfitano, A. Adenovirus vector induced innate immune responses: Impact upon efficacy and toxicity in gene therapy and vaccine applications. *Virus Res.* **132**, 1–14 (2008).
7. Zhu, J., Huang, X. & Yang, Y. Innate immune response to adenoviral vectors is mediated by both toll-like receptor-dependent and -independent pathways. *J. Virol.* **81**, 3170–3180 (2007).
8. Yamaguchi, T. et al. Role of MyD88 and TLR9 in the innate immune response elicited by serotype 5 adenoviral vectors. *Hum. Gene Ther.* **18**, 753–762 (2007).
9. Lam, E., Stein, S. & Falck-Pedersen, E. Adenovirus detection by the cGAS/STING/TBK1 DNA sensing cascade. *J. Virol.* **88**, 974–981 (2014).
10. Yamaguchi, T. et al. Induction of type i interferon by adenovirus-encoded small RNAs. *Proc. Natl. Acad. Sci. U. S. A.* **107**, 17286–17291 (2010).
11. Marquez-Martinez, S., Vijayan, A., Khan, S. & Zahn, R. Cell entry and innate sensing shape adaptive immune responses to adenovirus-based vaccines. *Curr. Opin. Immunol.* **80**, 102282 (2023).
12. Tatsis, N. & Ertl, H. C. J. Adenoviruses as vaccine vectors. *Mol. Ther.* **10**, 616–629 (2004).
13. Scarsella, L. et al. Advances of recombinant adenoviral vectors in preclinical and clinical applications. *Viruses* **16**, 377 (2024).
14. Bergelson, J. M. et al. Isolation of a common receptor for Coxsackie B viruses and adenoviruses 2 and 5. *Science* **275**, 1320–1323 (1997).
15. Wickham, T. J., Mathias, P., Cheresh, D. A. & Nemerow, G. R. Integrins αvβ3 and αvβ5 promote adenovirus internalization but not virus attachment. *Cell* **73**, 309–319 (1993).
16. Shayakhmetov, D. M., Gaggar, A., Ni, S., Li, Z.-Y. & Lieber, A. Adenovirus binding to blood factors results in liver cell infection and hepatotoxicity. *J. Virol.* **79**, 7478–7491 (2005).
17. Xu, Z. et al. Coagulation factor X shields adenovirus type 5 from attack by natural antibodies and complement. *Nat. Med.* **19**, 452–457 (2013).
18. Lopez-Gordo, E., Denby, L., Nicklin, S. A. & Baker, A. H. The importance of coagulation factors binding to adenovirus: Historical perspectives and implications for gene delivery. *Expert Opin. Drug Deliv.* **11**, 1795–1813 (2014).
19. Waddington, S. N. et al. Adenovirus Serotype 5 Hexon Mediates Liver Gene Transfer. *Cell* **132**, 397–409 (2008).
20. Shayakhmetov, D. M., Eberly, A. M., Li, Z.-Y. & Lieber, A. Deletion of penton RGD motifs affects the efficiency of both the internalization and the endosome escape of viral particles containing adenovirus serotype 5 or 35 fiber knobs. *J. Virol.* **79**, 1053–1061 (2005).
21. Dicks, M. D. J. et al. Differential immunogenicity between HAdV-5 and chimpanzee adenovirus vector ChAdOx1 is independent of fiber and penton RGD loop sequences in mice. *Sci. Rep.* **5**, 16756 (2015).
22. Akiyama, M. et al. Ablating CAR and integrin binding in adenovirus vectors reduces nontarget organ transduction and permits sustained bloodstream persistence following intraperitoneal administration. *Mol. Ther.* **9**, 218–230 (2004).
23. Bradshaw, A. C. et al. Biodistribution and inflammatory profiles of novel penton and hexon double-mutant serotype 5 adenoviruses. *J. Control. Release* **164**, 394–402 (2012).
24. Alba, R. et al. Biodistribution and retargeting of FX-binding ablated adenovirus serotype 5 vectors. *Blood* **116**, 2656–2664 (2010).
25. Mizuguchi, H. CAR- or alphav integrin-binding ablated adenovirus vectors, but not fiber-modified vectors containing RGD peptide, do not change the systemic gene transfer properties in mice. *Gene Ther.* **9**, 769–776 (2002).
26. Alba, R. et al. Identification of coagulation factor (F)X binding sites on the adenovirus serotype 5 hexon: Effect of mutagenesis on FX interactions and gene transfer. *Blood* **114**, 965–971 (2009).
27. Sakurai, F. et al. Efficient detection of human circulating tumor cells without significant production of false-positive cells by a novel conditionally replicating adenovirus. *Mol. Ther. Methods Clin. Dev.* **3**, 16001 (2016).
28. Irigoyen, M. et al. Tgfbi expression is associated with a better response to chemotherapy in NSCLC. *Mol. Cancer* **9**, 130 (2010).
29. Juratli, M. A. et al. Integrin α2 and β1 cross-communication with mTOR/AKT and the CDK-cyclin axis in hepatocellular carcinoma cells. *Cancers* **14**, 2430 (2022).

30. Asaoka, K., Tada, M., Sawamura, Y., Ikeda, J. & Abe, H. Dependence of efficient adenoviral gene delivery in malignant glioma cells on the expression levels of the Coxsackievirus and adenovirus receptor. *J. Neurosurg.* **92**, 1002–1008 (2000).
31. Koizumi, N. et al. Efficient gene transfer by fiber-mutant adenoviral vectors containing RGD peptide. *Biochim. Biophys. Acta* **1568**, 13–20 (2001).
32. Kalyuzhniy, O. et al. Adenovirus serotype 5 hexon is critical for virus infection of hepatocytes in vivo. *Proc. Natl. Acad. Sci. U. S. A.* **105**, 5483–5488 (2008).
33. Hassan, A. O. et al. A single-dose intranasal ChAd vaccine protects upper and lower respiratory tracts against SARS-CoV-2. *Cell* **183**, 169-184.e13 (2020).
34. Hassan, A. O. et al. An intranasal vaccine durably protects against SARS-CoV-2 variants in mice. *Cell Rep.* **36**, 109452 (2021).
35. Fonseca, J. A. et al. A prime-boost immunization regimen based on a simian adenovirus 36 vectored multi-stage malaria vaccine induces protective immunity in mice. *Vaccine* **35**, 3239–3248 (2017).
36. Pulendran, B. & Ahmed, R. Immunological mechanisms of vaccination. *Nat. Immunol.* **12**, 509–517 (2011).
37. Ols, S. et al. Route of vaccine administration alters antigen trafficking but not innate or adaptive immunity. *Cell Rep.* **30**, 3964-3971. e7 (2020).
38. Iwasaki, A. & Omer, S. B. Why and how vaccines work. *Cell* **183**, 290–295 (2020).
39. Hirsch, E., Lohikangas, L., Gullberg, D., Johansson, S. & Fässler, R. Mouse myoblasts can fuse and form a normal sarcomere in the absence of beta1 integrin expression. *J. Cell Sci.* **111**, 2397–2409 (1998).
40. Hirsch, E. et al. Alpha v integrin subunit is predominantly located in nervous tissue and skeletal muscle during mouse development. *Dev. Dyn.* **201**, 108–120 (1994).
41. Nalbantoglu, J., Pari, G., Karpati, G. & Holland, P. C. Expression of the primary coxsackie and adenovirus receptor is downregulated during skeletal muscle maturation and limits the efficacy of adenovirus-mediated gene delivery to muscle cells. *Hum. Gene Ther.* **10**, 1009–1019 (1999).
42. Onishi, R. et al. Development of a novel adenovirus serotype 35 vector vaccine possessing an RGD peptide in the fiber knob and the E4 orf 4, 6, and 6/7 regions of adenovirus serotype 5. *Int. J. Pharm.* **662**, 124480 (2024).
43. Wang, Y. et al. Mucosal adenovirus vaccine Ad5-XBB.1.5 boosting elicits nasal IgA and transiently prevents JN.1 wave infection for less than 6 months in real-world settings. *hLife* **3**, 433–447 (2025).
44. Xing, M. et al. An intranasal combination vaccine induces systemic and mucosal immunity against COVID-19 and influenza. *NPJ Vaccines* **9**, 64 (2024).
45. Wu, S. et al. A single dose of an adenovirus-vectored vaccine provides protection against SARS-CoV-2 challenge. *Nat. Commun.* **11**, 4081 (2020).
46. Wang, L. et al. Mucosal boosting increases protective efficacy of an influenza vaccine in mice. *iScience* **28**, 112721 (2025).
47. Jacob-Dolan, C. et al. Adenovirus and mRNA vaccines as well as mucosal boosting improve protective efficacy against influenza virus challenge in macaques. *Sci. Transl. Med.* **17**, eadu7646 (2025).
48. Gagne, M. et al. Mucosal adenovirus vaccine boosting elicits IgA and durably prevents XBB.1.16 infection in nonhuman primates. *Nat. Immunol.* **25**, 1913–1927 (2024).
49. Lasaro, M. O. & Ertl, H. C. J. New insights on adenovirus as vaccine vectors. *Mol. Ther.* **17**, 1333–1339 (2009).
50. Kaech, S. M. & Ahmed, R. Memory CD8+ T cell differentiation: Initial antigen encounter triggers a developmental program in naïve cells. *Nat. Immunol.* **2**, 415–422 (2001).
51. Yong, L., Hutchings, C., Barnes, E., Klenerman, P. & Provine, N. M. Distinct requirements for CD4+ T cell help for immune responses induced by mRNA and adenovirus-vector SARS-CoV-2 vaccines. *Eur. J. Immunol.* **55**, e202451142 (2025).
52. Swarnalekha, N. et al. T resident helper cells promote humoral responses in the lung. *Sci. Immunol.* **6**, 6808 (2021).
53. Provine, N. M. et al. Longitudinal requirement for CD4+ T cell help for adenovirus vector-elicited CD8+ T cell responses. *J. Immunol.* **192**, 5214–5225 (2014).
54. Li, J. X. et al. Safety and immunogenicity of heterologous boost immunisation with an orally administered aerosolised Ad5-nCoV after two-dose priming with an inactivated SARS-CoV-2 vaccine in Chinese adults: A randomised, open-label, single-centre trial. *Lancet Respir. Med.* **10**, 739–748 (2022).
55. Tukhvatulin, A. I. et al. Immunogenicity and protectivity of intranasally delivered vector-based heterologous prime-boost COVID-19 vaccine Sputnik V in mice and non-human primates. *Emerg. Microbes Infect.* **11**, 2229–2247 (2022).
56. Sunagar, R., Prasad, S. D., Ella, R. & Vadrevu, K. M. Preclinical evaluation of safety and immunogenicity of a primary series intranasal COVID-19 vaccine candidate (BBV154) and humoral immunogenicity evaluation of a heterologous prime-boost strategy with COVAXIN (BBV152). *Front. Immunol.* **13**, 1063679 (2022).
57. Dicks, M. D. J. et al. A novel chimpanzee adenovirus vector with low human seroprevalence: Improved systems for vector derivation and comparative immunogenicity. *PLoS One* **7**, e40385 (2012).
58. Baker, A. T. et al. ChAdOx1 interacts with CAR and PF4 with implications for thrombosis with thrombocytopenia syndrome. *Sci. Adv.* **7**, eabl8213 (2021).
59. Greinacher, A. et al. Thrombotic thrombocytopenia after ChAdOx1 nCov-19 vaccination. *N. Engl. J. Med.* **384**, 2092–2101 (2021).
60. Schultz, N. H. et al. Thrombosis and thrombocytopenia after ChAdOx1 nCoV-19 vaccination. *N. Engl. J. Med.* **384**, 2124–2130 (2021).
61. Muir, K.-L., Kallam, A., Koepsell, S. A. & Gundabolu, K. Thrombotic thrombocytopenia after Ad26.COV2.S vaccination. *N. Engl. J. Med.* **384**, 1964–1965 (2021).
62. Chen, Y. C. et al. Shear-dependent platelet aggregation by ChAdOx1 nCoV-19 vaccine: A novel biophysical mechanism for arterial thrombosis. *Blood* **146**, 496–503 (2025).
63. Murakami, S. et al. Interaction of penton base Arg-Gly-Asp motifs with integrins is crucial for adenovirus serotype 35 vector transduction in human hematopoietic cells. *Gene Ther.* **14**, 1525–1533 (2007).
64. Pillon, N. J., Bilan, P. J., Fink, L. N. & Klip, A. Cross-talk between skeletal muscle and immune cells : Muscle-derived mediators and metabolic implications. *Am. J. Physiol. Endocrinol. Metab.* **304**, E453–E465 (2013).
65. Mizuguchi, H. & Kay, M. A. A simple method for constructing E1- and E1/E4-deleted recombinant adenoviral vectors. *Hum. Gene Ther.* **10**, 2013–2017 (1999).
66. Mizuguchi, H. et al. A simplified system for constructing recombinant adenoviral vectors containing heterologous peptides in the HI loop of their fiber knob. *Gene Ther.* **8**, 730–735 (2001).
67. Mizuguchi, H. & Kay, M. A. Efficient construction of a recombinant adenovirus vector by an improved in vitro ligation method. *Hum. Gene Ther.* **9**, 2577–2583 (1998).
68. Maizel, J. V., White, D. O. & Scharff, M. D. The polypeptides of adenovirus: I. Evidence for multiple protein components in the virion and a comparison of types 2, 7A, and 12. *Virology* **36**, 115–125 (1968).
69. Shimizu, K., Sakurai, F., MacHitani, M., Katayama, K. & Mizuguchi, H. Quantitative analysis of the leaky expression of adenovirus genes in cells transduced with a replication-incompetent adenovirus vector. *Mol. Pharm.* **8**, 1430–1435 (2011).
70. Ono, R. et al. Oncolytic adenovirus serotype 35 mediated tumor growth suppression via efficient activation of antitumor immunity. *J. Immunother. Cancer.* **13**, e006558 (2025).

Acknowledgements

We thank Eiko Sakai and Yukiko Toba-Ueyama (Graduate School of Pharmaceutical Sciences, The University of

Osaka, Osaka, Japan) for their support.

Author contributions

Rika Onishi: Methodology, Investigation, Formal analysis, Writing—original draft preparation, Writing—review & editing. Aoi Shiota: Methodology, Investigation, Formal analysis. Hayato Nakatani: Methodology, Investigation. Masashi Tachibana: Methodology, Supervision. Kahori Shimizu: Methodology, Supervision. Toshiro Hirai: Methodology. Yasuo Yoshioka: Methodology. Fuminori Sakurai: Conceptualization, Supervision, Writing—review & editing. Hiroyuki Mizuguchi: Conceptualization, Supervision, Writing—review & editing, Funding acquisition.

Funding

This study was supported by a Grant-in-Aid for Scientific Research (A) (23H00552) from the Ministry of Education, Culture, Sports, Sciences, and Technology of Japan, the Platform Project for Supporting Drug Discovery and Life Science Research (Basis for Supporting Innovative Drug Discovery and Life Science Research (BINDS)) from the AMED (JP25ama121052 and JP25ama121054). This study was partially supported by BIKEN Foundation. This work was conducted as part of "The Nippon Foundation—Osaka University Project for Infectious Disease Prevention". Rika Onishi and Aoi Shiota are a research fellow of the Japan Society for the Promotion of Science.

Declarations

Competing interests

The authors declare no competing interests.

Ethics approval

All of the animal experiments performed in this study were approved by the Animal Experiment Committee of The University of Osaka (approval no. 28–3-3). All procedures were performed in accordance with the ethical standards of the Guide for the Care and Use of Laboratory Animals published by the National Institutes of Health, and ARRIVE guidelines.

Additional information

Supplementary Information The online version contains supplementary material available at https://doi.org/10.1038/s41598-026-49127-5.

Correspondence and requests for materials should be addressed to F.S. or H.M.

Reprints and permissions information is available at www.nature.com/reprints.

Publisher's note Springer Nature remains neutral with regard to jurisdictional claims in published maps and institutional affiliations.

Open Access This article is licensed under a Creative Commons Attribution-NonCommercial-NoDerivatives 4.0 International License, which permits any non-commercial use, sharing, distribution and reproduction in any medium or format, as long as you give appropriate credit to the original author(s) and the source, provide a link to the Creative Commons licence, and indicate if you modified the licensed material. You do not have permission under this licence to share adapted material derived from this article or parts of it. The images or other third party material in this article are included in the article's Creative Commons licence, unless indicated otherwise in a credit line to the material. If material is not included in the article's Creative Commons licence and your intended use is not permitted by statutory regulation or exceeds the permitted use, you will need to obtain permission directly from the copyright holder. To view a copy of this licence, visit http://creativecommons.org/licenses/by-nc-nd/4.0/.

© The Author(s) 2026